

Meta Reinforcement Learning for Resource Allocation in Unmanned Aerial Vehicles with MIMO Visible Light Communication

Hosein Zarini[†], Amir Mohammadi^{*}, Maryam Farajzadeh Dehkordi^{**},
Mohammad Robat Mili[§], Bardia Safaei[†], Ali Movaghar[†] and Merouane Debbah^{††}

[†]Sharif University of Technology, Tehran, Iran

^{*}Universidad Miguel Hernandez de Elche, Alicante, Spain

^{**}George Mason University, VA, United States of America

[§]Pasargad Institute for Advanced Innovative Solutions (PIAIS), Tehran, Iran

^{††}Khalifa University of Science and Technology, Abu Dhabi, United Arab Emirates

Abstract—This paper centers around a multiple-input-multiple-output (MIMO) visible light communication (VLC) system, where an unmanned aerial vehicle (UAV) benefits from a light emitting diode (LED) array to serve photo-diode (PD)-equipped users for illumination and communication simultaneously. Concerning the battery limitation of the UAV and considerable energy consumption of the LED array, a hybrid dimming control scheme is devised at the UAV that effectively controls the number of glared LEDs and thereby mitigates the overall energy consumption. To assess the performance of this system, a radio resource allocation problem is accordingly formulated for jointly optimizing the motion trajectory, transmit beamforming and LED selection at the UAV, assuming that channel state information (CSI) is partially available. By reformulating the optimization problem in Markov decision process (MDP) form, we propose a soft actor-critic (SAC) mechanism that captures the dynamics of the problem and optimizes its parameters. Additionally, regarding the frequent mobility of the UAV and thus remarkable rearrangement of the system, we enhance the trained SAC model by integrating a meta-learning strategy that enables more adaptation to system variations. According to simulations, upgrading a single-LED UAV by an array of 10 LEDs, exhibits 47% and 34% improvements in data rate and energy efficiency, albeit at the expense of 8% more power consumption.

Index Terms—Multiple-input-multiple-output (MIMO), visible light communication (VLC), unmanned aerial vehicle (UAV), resource allocation, channel state information (CSI), soft actor-critic (SAC), meta-learning.

I. INTRODUCTION

Visible light communication (VLC) is anticipated to address the limitations of existing radio-frequency (RF) communication systems. In VLC transmissions, signal propagation relies on a light-emitting diode (LED) at transmitter, while signal decoding is performed using a photo-diode (PD) at receiver [1]. This technology, in fact, offers a unique advantage by combining illumination and communication simultaneously. Thanks to this multi-functionality, VLC systems have experienced remarkable advancements and evolved within a few years. Not long ago, the deployment of multiple LEDs in a LED array introduced the concept of multiple-input-multiple-output (MIMO) in VLC systems, accompanied by significant

improvements in network data rate and coverage [2]–[4]. Later, the application of VLC band introduced in aerial communication platforms by equipping unmanned aerial vehicles (UAVs) with a single-LED. This achievement promised even better coverage and flexible maneuverability over terrestrial VLC systems [5]. To date, a plethora of literature have studied VLC-enabled UAV-based networks from network coverage [6], data rate [7] and energy efficiency [8] standpoints. *Nonetheless, our investigations reveal that despite tremendous gain brought by MIMO-VLC [2]–[4], this technology has never been studied for the UAV in the existing art hitherto [5]–[8].*

This paper is dedicated to filling the aforementioned research gap by proposing a resource allocation mechanism to evaluate the performance a UAV equipped with a LED array, as a UAV-MIMO-VLC system. This study faces two design challenges: *i*) LED arrays consume more power compared to a single-LED and their deployment on a UAV with strictly battery limitation raises an undeniable concern. *ii*) Considerable dynamism of the UAV-MIMO-VLC system originated from frequent motion of the UAV poses a challenge for real-time and on-demand resource allocation. Toward addressing these challenges, this treatise proposes the following contributions:

- Unlike [5]–[8] that investigated a single-LED UAV, our work centers around a UAV that is equipped with a LED array. In light of the UAV battery constraint and notable energy demand of the LED array, we adopt a hybrid dimming control strategy [9] that jointly manages the direct current (DC)-bias level and the number of glaring LEDs at the LED array to substantially reduce its energy consumption.
- The performance of this system is evaluated under the practical assumption of imperfect channel state information (CSI) at the UAV. Specifically, we formulate a radio resource management problem aimed at minimizing the UAV power consumption based on its trajectory design, beamforming control and LED selection, simultaneously.

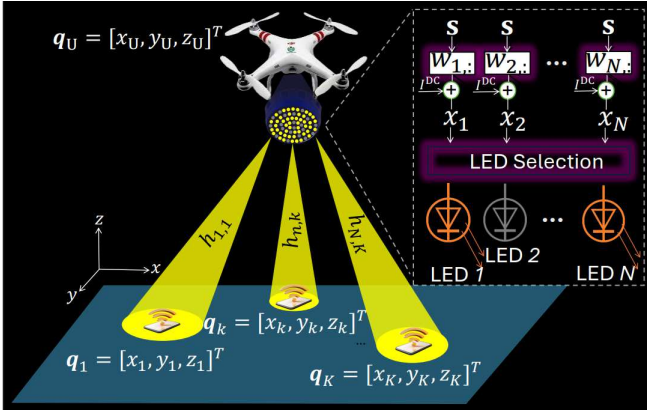


Fig. 1: A UAV-MIMO-VLC system.

We present a real-time and robust resource allocation approach using a soft actor-critic (SAC) mechanism, which involves reformulation of the problem as a Markov decision process (MDP). This approach effectively captures the problem's dynamics and optimizes its parameters.

- What's more, to address the swift reconfiguration of the system, initiated by frequent mobility of the UAV, we augment the trained SAC model with a meta-learning strategy. This integration indeed enhances the model adaptability to system variations and outperforms evaluation metrics compared to the similar resource allocation method in [5].
- It is numerically revealed that compared to the single-LED UAV [5]–[8], the proposed UAV equipped with a LED array composed of 10 LEDs achieves 47% and 34% advancements in data rate and energy efficiency, respectively. Nevertheless, this progress comes with a marginal trade-off, with an additional 8% more power consumption incurred.

II. SYSTEM MODEL AND PROBLEM FORMULATION

In this section, we elaborate the UAV-MIMO-VLC system setting and formulate an optimization problem for evaluating the performance of this system.

A. Signal Model

Downlink transmission of a visible light communication (VLC) system is studied as depicted in Fig. 1, within which an array of LEDs is patched to a rotary-wing unmanned aerial vehicle (UAV) for the illumination and communication purpose at the same time. In specific, the LED array includes a set $\mathcal{N} = \{1, 2, \dots, N\}$ of N LEDs deployed at the UAV to serve a set $\mathcal{K} = \{1, 2, \dots, K\}$ of K randomly positioned users, each equipped with a single photo-detector (PD). The LEDs are supposed to be independently modulated via separate drivers, yet all are deployed at the UAV as a central controller that collects channel feedback and performs resource management. Let $\mathbf{s} = [s_1, s_2, \dots, s_N] \in \mathbb{R}^{N \times 1}$ denote the data symbol vector, intended for all user, such that $s_k \in [-1, 1]$ specifies the data symbol for the user k and $\mathbb{E}\{|s_k|^2\} = 1 \forall k \in \mathcal{K}$. Also, let us define a transmit precoding matrix $\mathbf{W} = [\mathbf{w}_1, \mathbf{w}_2, \dots, \mathbf{w}_K] \in$

$\mathbb{R}^{N \times K}$ with $\mathbf{w}_k = [w_{1,k}, w_{2,k}, \dots, w_{N,k}] \in \mathbb{R}^{N \times 1}$ being the beamforming vector for the user k . Designing an efficient precoding scheme significantly helps controlling the inter-user interference. Without loss of generality, we assume a linear precoding for data symbols [5]. In optical communications, generated signals have to be real-valued and non-negative. This requirement is covered by direct current (DC)-biased modulation, through which the brightness of LEDs and average optical power are also determined. Taking this fact into consideration, the transmit signal vector of all LEDs can be expressed as $\mathbf{x} = \sum_{k=1}^K \mathbf{w}_k \mathbf{s}_k + \mathbf{I}^{\text{DC}}$, where the DC bias $\mathbf{I}^{\text{DC}} = [I_1^{\text{DC}}, I_2^{\text{DC}}, \dots, I_N^{\text{DC}}] \in \mathbb{R}^{N \times 1}$ has been incorporated so as to ensure that the amplitude of the transmit signal vector resides within the non-negative range of LEDs. Besides, for the sake of uniformity of illumination in indoor environments, the DC bias is assumed to be the same for all the LEDs [9]. On this basis, the LED indices can be simply removed, which results in $I_n^{\text{DC}} = I^{\text{DC}} \forall n \in \mathcal{N}$ and $\mathbf{I}^{\text{DC}} = I^{\text{DC}}$. Accordingly, the transmit signal of a typical LED n , i.e., x_n satisfies $-\sum_{k=1}^K |w_{n,k}| + I^{\text{DC}} \leq x_n \leq \sum_{k=1}^K |w_{n,k}| + I^{\text{DC}} \forall n \in \mathcal{N}$. All LEDs, however, work within their dynamic ranges to avoid signal clipping. This consideration poses a constraint for the transmit beamforming vector as $\sum_{k=1}^K |\mathbf{w}_k| \leq \min(I^{\text{DC}} - I_l, I_h - I^{\text{DC}}) \forall n \in \mathcal{N}$, with I_l and I_h being the lower and upper bound of the LED driver current, respectively.

B. Channel Model

For a typical VLC receiver, a line-of-sight (LoS) link constitutes about 95% of the total received power, such that at least 7 dB difference is roughly observed between the received power for the LoS link and that for the most dominant non-line-of-sight (NLoS) one [5]. In light of this fact, by neglecting the NLoS links, we only take the LoS links into account in our work. Suppose that the UAV and the typical user k are located at the coordinates of $\mathbf{q}_U = [x_U, y_U, z_U]^T$ and $\mathbf{q}_k = [x_k, y_k, z_k]^T$, respectively. In comparison with the distance between the UAV and ground users, the distance between the LEDs deployed at the UAV is trivial. Hence, a unified (and not per LED) coordinate is considered for the UAV. So, the direct distance between the user k and the UAV can be calculated as: $d_{U,k} = \sqrt{(x_U - x_k)^2 + (y_U - y_k)^2 + (z_U - z_k)^2}$. However, the channel condition may significantly differ between two adjacent LEDs, regarding their transmission semi-angles. We denote the optical channel gain from the LED n to the user k by $h_{n,k} \in \mathbb{R}$, which is modelled as: $h_{n,k} = \frac{(m+1)A_k}{2\pi d_{U,k}^2} G^{\text{VLC}}(\psi_{n,k}) \cos^m(\phi_{n,k}) \cos(\psi_{n,k})$ for $0 \leq \psi_{n,k} \leq \Psi_c$, and $h_{n,k} = 0$, otherwise. In such a channel modelling, the detection area of the PD at the user k is defined by A_k . Besides, $m = -\frac{\ln 2}{\ln(\cos \Phi_{1/2})}$ stands for the order of Lambertian emission with $\Phi_{1/2}$ being the half-power semi-angle of the LED. The angles of incidence and irradiance between the LED n and the user k , are respectively represented by $\psi_{n,k}$ and $\phi_{n,k}$, such that $\cos(\psi_{n,k}) = \cos(\phi_{n,k}) = d_{U,k} / (z_U - z_k)$. Moreover, Ψ_k specifies the field of vision (FOV) semi-angle at the user k and $G^{\text{VLC}}(\psi_{n,k})$ indicates the gain of the optical concentrator,

with $q \geq 0$ introducing the internal refractive index. However, the availability of perfect CSI is an ideal assumption, which leads to remarkable performance degradation. Especially in VLC systems, where optical lightweight signals are heavily prone to environmental obstacles or reflections, the practical consideration of imperfect CSI at the transmitter (the UAV in our scenario) would provide the system with a realistic performance analysis [10]. We model the imperfect channel between the LED n and user k as $\hat{h}_{n,k} = h_{n,k} + \epsilon_{n,k}$, wherein $\epsilon_{n,k}$, represents the estimation error within a bounded region. This error is defined as $|\epsilon_{n,k}| \leq \delta$, where δ corresponds to the channel uncertainty radius and is assumed to be a small constant.

C. Hybrid Dimming

As discussed earlier, the concept of hybrid dimming is a multi-domain dimming approach that exploits analog domain (AD) and spatial domain (SD) at the same time [9]. Thanks to invoking SD, only a subset of LEDs are glared, while the remaining become inactive. Hence, compared to conventional systems with digital dimming (DD), the power consumption of a hybrid dimming-enabled system is significantly lower. For equipping UAVs to optical multiple-input-multiple-output (MIMO) technology with a LED array therefore, a hybrid dimming control scheme is indispensable regarding the strict energy limitation of the UAV. To this purpose, let us introduce a binary LED selection matrix $\mathbf{A} = \text{diag}(\mathbf{a}) \in \{0, 1\}^{N \times N}$, with $\mathbf{a} = [a_1, \dots, a_N]^T \in \{0, 1\}^{N \times 1}$, such that $a_n=1$ specifies the glared state of the LED n , whereas $a_n=0$ delineates that it is inactive. Accordingly, the number of active LEDs can be calculated as $N_a = \sum_{n=1}^N a_n$. By adopting a hybrid dimming control mechanism, the signal benefits from both analog and spatial domains simultaneously. So, the uniform DC-bias level (corresponded to AD) and the number of glared LEDs (corresponded to SD) need to be jointly adjusted. To do so, we firstly define a target dimming level denoted by η with a predetermined value. Given η then, the number of glared (actual working) LEDs for SD can be simply rounded-off as $N_a = \lceil \eta N \rceil$. On this basis, the uniform DC-bias level I^{DC} for AD will be acquired as [9]: $I^{\text{DC}} = \frac{\eta N (I_0 - I_l)}{N_a} + I_l$, in which $I_0 = \frac{I_l + I_h}{2}$ defines the original DC-bias for AD, when all N LEDs are glared and $\eta = 100\%$ dimming level is set. By determining (N_a) thus far, we are aware of how many LEDs are glared in fact. However, it is required to exactly specify which LEDs at the LED array have to be active. This will be clarified by optimizing the binary LED selection matrix \mathbf{A} in a network-wide optimization problem, which will be mathematically formulated in upcoming subsections.

D. Trajectory Control and Power Consumption for UAV

For a durable and efficient aerial communication, it is required to meticulously trace the flight trajectory and power consumption of UAV.

Trajectory Control: Concerning the frequent mobility of the UAV and for the sake of analysis, we discretize its overall

flight time duration T to a set $\mathcal{L} = \{0, 1, 2, \dots, L\}$ with L time slots, each occupying a duration of τ , such that $T = L\tau$. The duration of time slots is adopted to be sufficiently small, within which the configuration of the network is supposed to remain static and the optical channels follow a quasi-static model. Within a typical time slot l , the UAV is assumed to fly with the velocity of $\mathbf{v}_U(l) = [v_U^x(l), v_U^y(l), v_U^z(l)]^T \in \mathbb{R}^{3 \times 1}$, such that its initial and final positions are the same, i.e., it returns to the beginning position at the end of the last time slot L for recharging. The flight restrictions of the UAV pose some constraints to the system. First, $\mathbf{q}_U(l+1) = \mathbf{q}_U(l) + \mathbf{v}_U(l)\tau$ determines its next location with respect to (w.r.t.) the movement velocity; Through $\mathbf{q}_U[0] = \mathbf{q}_U[L] = \mathbf{q}_U^1$, we guarantee the comeback of the UAV to its initial location \mathbf{q}_U^1 at the end of the last time slot L ; We restrict the UAV flight to the minimum and maximum boundaries \mathbf{q}_{\min} and \mathbf{q}_{\max} as $\mathbf{q}_{\min} < \mathbf{q}_U(l) < \mathbf{q}_{\max}$; Finally, $\|\mathbf{v}_U(l+1) - \mathbf{v}_U(l)\| \leq a_{\max}\tau$ and $\|\mathbf{v}_U(l)\| \leq V_{\max}$ control the flight acceleration and velocity of the UAV by introducing the maximum flight acceleration a_{\max} and maximum flight velocity V_{\max} , respectively.

Power Consumption: The consumed power related to hovering of the UAV, categorized to blade power consumption P_b and induced power consumption P_i , can be modelled as [11]: $P_{\text{Hov}} = P_b + P_i$ where $P_b \triangleq \frac{\rho}{8} \zeta \delta A_U \Omega_U^3 R_U^3$ and $P_i \triangleq (1 + \iota) \frac{W_U^{3/2}}{\sqrt{2\zeta A_U}}$. Specifically, P_{Hov} includes the profile

$$P_{\text{Hov}} = \underbrace{\left(1 + \frac{3\|\mathbf{v}_U\|^2}{\Omega_U^2 R_U^2}\right) P_b}_{\text{blade profile}} + \underbrace{\left(\sqrt{1 + \frac{\|\mathbf{v}_U\|^4}{4v_{\text{UI}}^4}} - \frac{\|\mathbf{v}_U\|^2}{2v_{\text{UI}}^2}\right) P_i}_{\text{induced}} + \underbrace{\frac{1}{2} d_U \zeta \delta A_U \|\mathbf{v}_U\|^3}_{\text{parasite}},$$

in which v_{UI} specifies the mean rotor induced velocity in hover, while d_U denotes the fuselage drag ratio. Finally, the total consumed power of the system can be calculated as: $P^{\text{Tot}} = \zeta \sum_{n=1}^N \sum_{k=1}^K \mathbf{a} w_{n,k} + \varphi N_a I^{\text{DC}} + P^{\text{Cir}} + P^{\text{Prop}}$, with ζ being the amplifier efficiency factor, φ determining the conversion factor, as well as P^{Cir} designating the consumed power of switch and control circuit modules at the UAV.

E. Transmission Protocol

We adopt the power-domain non-orthogonal multiple access (NOMA) scheme for enabling massive access in the system. Suppose $|\mathbf{h}_1^H \mathbf{w}_1|^2 \leq |\mathbf{h}_2^H \mathbf{w}_2|^2 \leq \dots \leq |\mathbf{h}_K^H \mathbf{w}_K|^2$ as the descending order of the channel coefficients. Then, the instantaneous

received data rate of the user k can be expressed as:

$$R_k(\mathbf{W}, \mathbf{A}, \mathbf{Q}) = \log_2 \left(1 + \frac{|\mathbf{h}_k^H \mathbf{A} \mathbf{w}_k|^2}{\sum_{i=k+1}^K |\mathbf{h}_k^H \mathbf{A} \mathbf{w}_i|^2 + \sigma_k^2} \right), \quad (1)$$

where $\mathbf{h}_k = [h_{k,1}, h_{k,2}, \dots, h_{k,N}]^T$ denotes the channel vector of the user k .

F. Problem Formulation

We aim to jointly optimize the network resources $\{\mathbf{W}, \mathbf{Q} = \{\mathbf{q}_U, \mathbf{v}_U\}, \mathbf{A}\}$, such that the power consumption of the UAV is minimized and the UAV-MIMO-VLC system requirements are met. Mathematically, this problem is formulated as follows:

$$\mathcal{P}_1 : \min_{\mathbf{W}, \mathbf{A}, \mathbf{Q}} P^{\text{Tot}} \quad (2a)$$

$$\text{s.t. } C_1 : R_k(\mathbf{w}, \mathbf{A}, \mathbf{Q}) \geq R_{\min}, \quad \forall k \in \mathcal{K}, \quad (2a)$$

$$C_2 : P^{\text{Tot}} \leq P_{\max}, \quad (2b)$$

$$C_3 : \sum_{k=1}^K |\mathbf{w}_k| \leq \min(I^{\text{DC}} - I_l, I_h - I^{\text{DC}}), \quad \forall n \in \mathcal{N}, \quad (2c)$$

$$C_4 : \mathbf{q}_U(l+1) = \mathbf{q}_U(l) + \mathbf{v}_U(l) \tau, \quad \forall l \in \mathcal{L}, \quad (2d)$$

$$C_5 : \mathbf{q}_{\min} < \mathbf{q}_U(l) < \mathbf{q}_{\max}, \quad \forall l \in \mathcal{L}, \quad (2e)$$

$$C_6 : \|\mathbf{v}_U(l+1) - \mathbf{v}_U(l)\| \leq a_{\max} \tau, \quad \forall l \in \mathcal{L}, \quad (2f)$$

$$C_7 : \|\mathbf{v}_U(l)\| \leq V_{\max}, \quad \forall l \in \mathcal{L}, \quad (2g)$$

$$C_8 : \eta = \frac{N_a(I^{\text{DC}} - I_l)}{N(I_0 - I_l)} \times 100\%, \quad (2h)$$

$$C_9 : a_n \in \{0, 1\}, \quad \forall n \in \mathcal{N}, \quad (2i)$$

where the quality-of-service (QoS) requirement of all users (R_{\min}) is ensured in C_1 ; Constraint C_2 guarantees the transmit power budget of the UAV denoted by (P^{\max}); In C_3 , the dynamic range of all LEDs in the LED array is bounded; The flight restrictions of the UAV are described in C_4 - C_7 as discussed earlier; The target dimming level η is assured to be served in C_8 and C_9 finally defines the binary domain of the LED selection variable. By virtue of coupling variables drawn from both concrete and discrete domains and also incorporating non-convex constraint C_1 , this problem is non-convex. This observation renders \mathcal{P}_1 in a mixed-integer and nonlinear programming (MINLP) category, thereby classifying it as non-deterministic polynomial-time hardness (NP-hard). Unlike classical convex optimization-based solutions that offer intricate mathematical transformation to solve non-convex optimization problems, we propose a real-time and adaptive solution strategy to address \mathcal{P}_1 in the following section.

III. DETAILED DESCRIPTION OF THE PROPOSED SOLUTION STRATEGY

In this section, we reformulate (2) in MDP form and propose a Meta-SAC algorithm that integrates meta-learning with SAC. Compared to existing learning-driven resource allocation schemes mostly based on deep reinforcement learning (DRL) [5], the integration of meta-learning in our proposed method allows more adaptability into the system variations, thereby yielding a more real-time and flexible solution framework.

A. Reformulation of \mathcal{P}_1 in MDP form

We regard the UAV as the central controller, that roles as a DRL agent, interacting with the considered MIMO-VLC system as the DRL environment. The agent selects an action $\mathbf{a}(l) = \{\mathbf{W}(l), \mathbf{A}(l), \mathbf{Q}(l)\}$ in time step l based on the current state $\mathbf{s}(l) = \{\mathbf{h}_k\}$, $\forall k \in \mathcal{K}$, of the environment. We view $P_r(\mathbf{s}(l+1)|\mathbf{s}(l), \mathbf{a}(l))$ as the transition probability, representing the likelihood of transitioning to a new state $\mathbf{s}(l+1)$ from the current state of the environment $\mathbf{s}(l)$, when action $\mathbf{a}(l)$ is executed. Consequently, the environment transits to the new state $\mathbf{s}(l+1)$, and a reward function $Re(\mathbf{s}(l), \mathbf{a}(l))$ evaluates the efficacy of the chosen action. Formally, the reward function is defined as $Re(\mathbf{s}(l), \mathbf{a}(l)) = -P^{\text{Tot}}$, when C_1 - C_9 are met and $Re(\mathbf{s}(l), \mathbf{a}(l)) = 0$, otherwise.

B. Proposed Meta-SAC Algorithm

As a robust DRL algorithm tailored for ever-varying scenarios, SAC [12] is equipped with an agent whose objective is to determine the optimal policy π^* that maximizes a trade-off between the expected cumulative reward over time and a certain level of uncertainty or exploration in its actions, known as entropy. This trade-off measures the policy's randomness and can be formulated as: $\pi^* = \arg \max_{\pi} \mathbb{E}_{(\mathbf{s}(l), \mathbf{a}(l)) \sim \mathcal{P}} \left[\sum_{l=0}^{\infty} \gamma^l Re(\mathbf{s}(l), \mathbf{a}(l)) - \lambda \sum_{l=1}^{\infty} \gamma^l \log(\pi(\cdot|\mathbf{s}(l))) | \mathbf{s}(l) = \mathbf{s}(0), \mathbf{a}(l) = \mathbf{a}(0) \right]$, within which $\gamma \in (0, 1]$ designates the discount factor and \mathcal{P} stands for the transition probabilities. While effective in dynamic settings, where the training and testing environments of the DRL agent match, the traditional SAC, however, struggles to swiftly adjust to extremely updating conditions such as our case with a flying UAV. To tackle this situation, we introduce the Meta-SAC approach, by integrating the model-agnostic meta-learning (MAML) [13] with SAC. By doing so, Meta-SAC showcases superior generalization capabilities, enabling rapid adaptation to unseen upcoming environments [14]. Whereas the traditional SAC employs one actor and two critic networks, characterized by parameters ϕ , ψ_1 , and ψ_2 , respectively, meta-learning integrates one target actor (ϕ_e) and two target critic networks (ψ_{e1} and ψ_{e2}) to facilitate convergence.

The system model outlined in Section II incorporates random placements of the UAV and users in each instantiation. Consequently, the optimization problem \mathcal{P}_1 can be considered as a meta task scenario. Here, each task is defined by assuming distinct initial random locations for the UAV and users. Following the MAML approach [13], We define a meta task set $\mathcal{T}_t = \{t = 1, 2, \dots, T\}$, in which each task $t \in \mathcal{T}_t$ can be represented by the tuple $(\mathbf{s}_t(l), \mathbf{a}_t(l), \mathbf{s}_t(l+1), r_t(l))$, $\forall l \in \mathcal{L}$. Moreover, each task t possesses its specific replay buffer labeled as D_t , a support set D_t^{tr} as well as a query set D_t^{val} . The proposed Meta-SAC approach consists of two main stages, namely Meta-training and Meta-adaptation.

Meta-Training Phase: In the initial stage of meta-learning, both the actor and critic networks undergo training using

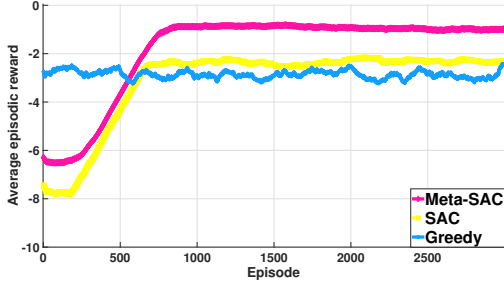


Fig. 2: Convergence behavior of the proposed resource allocation scheme.

a two-tier approach that encompasses individual-level and global-level updates [14]. At the former level, for each task t , the environment resets to initialize the state $s_t(0)$. Next, by adopting and applying the action $\mathbf{a}_t(l)$ in each time step l , the agent updates the environment to the new state $s_t(l+1)$ and the reward function $Re_t(l)$ evaluates the efficacy of the chosen action. Relying on adaptive moment estimation (ADAM) algorithm, subsequently, the actor and critic networks' parameters for each task t , denoted by $\hat{\phi}_t$, $\hat{\psi}_{1,t}$, and $\hat{\psi}_{2,t}$ respectively, are updated as: $\hat{\phi}_t = \arg \min_{\phi} \mathcal{L}_t^A(\phi, D_t^{rr})$, $\hat{\psi}_{1,t} = \arg \min_{\psi_1} \mathcal{L}_t^{C1}(\psi_1, D_t^{rr})$, and $\hat{\psi}_{2,t} = \arg \min_{\psi_2} \mathcal{L}_t^{C2}(\psi_2, D_t^{rr})$, with $\mathcal{L}_t^A(\phi, D_t^{rr})$, $\mathcal{L}_t^{C1}(\psi_1, D_t^{rr})$ and $\mathcal{L}_t^{C2}(\psi_2, D_t^{rr})$ quantifying the loss functions for the actor and critic networks, respectively. After applying individual-level updates of all tasks, the next step involves updating the global network parameters at the global-level. This process entails sampling a query set D_t^{val} randomly from the dataset D_t . Accordingly, the global network parameters are updated as: $\phi = \arg \min_{\phi} \sum_{t \in \mathcal{T}_t} \mathcal{L}_t^A(\hat{\phi}_t, D_t^{val})$, $\psi_1 = \arg \min_{\psi_1} \sum_{t \in \mathcal{T}_t} \mathcal{L}_t^{C1}(\hat{\psi}_{1,t}, D_t^{val})$ and $\psi_2 = \arg \min_{\psi_2} \sum_{t \in \mathcal{T}_t} \mathcal{L}_t^{C2}(\hat{\psi}_{2,t}, D_t^{val})$.

Meta-Adaptation Phase: During this stage, we insightfully initialize the parameters of the actor and critic networks relying on the trained parameters from the prior stage. In particular, we initialize Φ , Ψ_1 , and Ψ_2 , the parameters of the actor and critic networks, as $\Phi_0 = \phi$, $\Psi_{1,0} = \psi_1$, and $\Psi_{2,0} = \psi_2$, respectively. This stage already exploits another replay buffer D_{ada} , a batch of data \mathbb{D}_{ada} are randomly drawn from. Accordingly, the update rules for parameters of the actor and critic networks are respectively expressed as: $\Phi = \Phi - \beta_A \nabla_{\Phi} \mathcal{L}_A(\Phi, D_{ada})$, $\Psi_1 = \Psi_1 - \beta_{C1} \nabla_{\Psi_1} \mathcal{L}_{C1}(\Psi_1, D_{ada})$, and $\Psi_2 = \Psi_2 - \beta_{C2} \nabla_{\Psi_2} \mathcal{L}_{C2}(\Psi_2, D_{ada})$, with β_A , β_{C1} , and β_{C2} signifying the learning rates, the actor and critic networks are respectively trained with. The computational complexity for the Meta-SAC algorithm depends on the number of incorporated layers at the SAC [14].

IV. SIMULATION RESULTS

This section discusses the performance of the proposed UAV-MIMO-VLC system and the corresponding resource allocation scheme. To that end, three baselines are considered, including a single-LED corresponded to [7], as well as the baselines with $L=10$ and $L=20$ LEDs deployed at the UAV

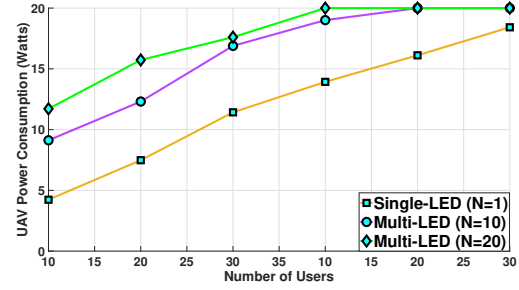


Fig. 3: Total power consumption of the UAV P^{Tot} versus the number of users K .

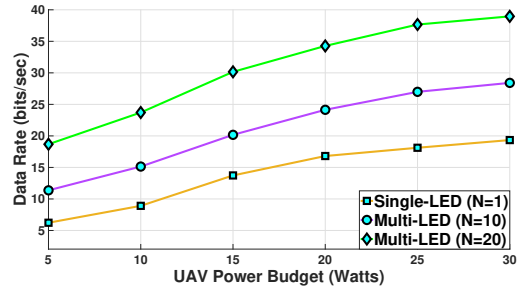


Fig. 4: Average achievable data rate versus power budget of the UAV P_{max} .

corresponded to our proposed system. The performance is assessed under three criteria, including power consumption of the UAV, as well as data rate and energy efficiency gained by the PD-equipped users. Simulations are performed with $K=30$ users, $R_{\min} = 2$ bits/s/Hz, $V_{\max} = 20$ m/s, $a_{\max} = 6$ m/s², $\mathbf{q}_{\max} = (150, 150, 100)$ m and $\tau = 1$ s. Other simulation parameters are summarized in Table I.

Fig. 2 showcases the convergence behaviour of the proposed resource allocation scheme. Specifically, about 65% lower power is consumed in average by the UAV while exploiting meta-learning. This achievement yields as the result of better adaptation of the proposed meta-learning-enabled resource allocation scheme to frequent variations of the UAV-MIMO-VLC system. Compared to the greedy resource allocation scheme, as seen, this gain is even more.

TABLE I: Simulation Parameters

Parameter	Value	Parameter	Value
Ψ_c	60°	n_R	1.5
$\phi_{1/2}$	60°	A_{VLC}	1 cm ²
I_h	10 mA	I_l	0 A
I_0	5 mA	ζ	1.2
φ	1	ζ'	1.225
N	10	P_{max}	20 W
ρ	0.012	δ	0.05
A_U	0.79	Ω_U	400
R_U	0.05	ι	1
W_U	100	ν_{UI}	7.2
d_U	0.3	R_{\min}	2 bits/s/Hz
V_{max}	10 m/s	a_{max}	6 m/s ²
\mathbf{q}_{max}	(150, 150, 100) m	τ	1s

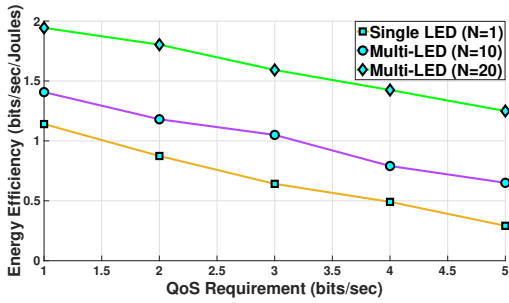


Fig. 5: Average achievable energy efficiency versus QoS requirement of users R_{\min} .

In Fig. 3, we have exhibited the effect of increasing the number of PD-equipped users on power consumption of the UAV. Evidently, by increasing the number of users, fulfilling their data rate requirement, as dictated in C_1 , induces more power consumption to the UAV. Quantitatively, a UAV with a LED array with $N=10$ LEDs consumes 40% more power in average, compared to a UAV employing a single-LED, when $K=10$. However, by increasing the number of users, the gap between the baselines diminishes as all baselines gradually approach the power budget of the UAV. For instance, when $K=30$, the gap between the aforementioned baselines falls under 8%. This observation underscores the effectiveness of the proposed UAV-MIMO-VLC system in dense networks. Another insight, drawn from Fig. 3 corresponds to the limited gap between the baselines with $N=10$ and $N=20$. This observation highlights the influence of the adopted hybrid dimming mechanism, which effectively controls the power consumption and promises the deployment of massive LED arrays to gain much higher data rates.

Fig. 4 depicts the impact of power budget of the UAV P_{\max} , when it is aimed to maximize the achievable data rate of the UAV-MIMO-VLC system. From this figure, we perceive that the proposed resource allocation scheme effectively exploits the available power budget, such that the inter-user interference in (1) is managed well and the overall achieved data rate of the network increases. More importantly, the single-LED baseline obtains much lower data rate, compared to the baselines with $N=10$ and $N=20$ LEDs. In average, around 47% gain is achieved, when comparing the baselines $N=10$ and $N=1$. This observation justifies that in comparison with a single-LED, the deployment of LED array at the UAV is much more cost effectiveness from the network data rate standpoint. Fig. 4 also reveals that the gap between the baselines $N=10$ and $N=20$ is much more than that between $N=1$ and $N=10$. Conclusively, one can argue that deploying massive LED arrays can better exploit the abundant capacity of the VLC band to fulfill the explosive data rate requirements of upcoming wireless networks.

Eventually, Fig. 5, analyzes the performance of the UAV-MIMO-VLC system, aimed at maximizing the overall energy efficiency, defined as a trade-off between the achievable data rate and power consumption of the system. In essence, assurance of more QoS requirement for users induces a user

fairness within the network, thereby degrades the overall achievable data rate of the network. Conversely, the UAV has to spend more transmit power to meet higher levels of QoS requirement. Under this argument, the more QoS requirement for users is guaranteed, the lower energy efficiency is achieved. Comparatively, it is clear that deploying a LED array with more number of LEDs at the UAV achieves much more energy efficiency, which underscores the effectiveness of the proposed UAV-MIMO-VLC system. For instance, in average, 34% better energy efficiency is achieved by the baseline with $N=10$, compared to the single-LED baseline $N=1$.

V. CONCLUSIONS

We proposed a UAV-MIMO-VLC system in this paper and evaluated its performance by an adaptive resource allocation framework. Through numerical results, we found that incorporating a LED array rather than a single-LED at the UAV, significantly improves the data rate and energy efficiency of the network, yet at the cost of increased power consumption.

REFERENCES

- [1] M. R. Maleki, M. R. Mili, M. R. Javan, N. Mokari and E. A. Jorswieck, "Multi-agent reinforcement learning trajectory design and two-stage resource management in CoMP UAV VLC networks," *IEEE Trans. Commun.*, vol. 70, no. 11, pp. 7464-7476, Nov. 2022.
- [2] K. Ying, H. Qian, R. J. Baxley and G. T. Zhou, "MIMO transceiver design in dynamic-range-limited VLC systems," *IEEE Photon. Technol. Letts.*, vol. 28, no. 22, pp. 2593-2596, Nov. 2016.
- [3] N. Chi, Y. Zhou, Y. Wei and F. Hu, "Visible light communication in 6G: advances, challenges, and prospects," *IEEE Veh. Technol. Mag.*, vol. 15, no. 4, pp. 93-102, Dec. 2020.
- [4] L. Zeng *et al.*, "High data rate multiple input multiple output (MIMO) optical wireless communications using white LED lighting," *IEEE J. Sel. Areas Commun.*, vol. 27, no. 9, pp. 1654-1662, Dec. 2009.
- [5] H. Zarini *et al.*, "Multiplexing eMBB and mMTC services over aerial visible light communications," in *Proc. IEEE Int. Conf. Commun., (ICC) Rome, Italy, 2023*, pp. 2655-2661.
- [6] D. N. Anwar, M. Peer, K. Lata, A. Srivastava and V. A. Bohara, "3-D deployment of VLC enabled UAV networks With energy and user mobility awareness," *IEEE Trans. Green Commun. Netw.*, vol. 6, no. 4, pp. 1972-1989, Dec. 2022.
- [7] P. Hou and N. Cen, "Sum-rate optimization for visible-light-Band UAV networks based on particle swarm optimization," in *Proc. IEEE 19th Ann. Consumer Commun. Netw. Conf. (CCNC)*, Las Vegas, NV, USA, 2022, pp. 163-168.
- [8] H. Ibraiwish, M. W. Eltokhey and M. -S. Alouini, "Energy efficient deployment of VLC-enabled UAV using particle Swarm optimization," *IEEE Open J Commun. Soc.*, vol. 5, pp. 553-565, 2024.
- [9] S. Javadi, *et al.*, "SLIPT in Joint Dimming Multi-LED OWC Systems with Rate Splitting Multiple Access," Feb. 2024.[Online]. Available: <https://arxiv.org/pdf/2402.16629v2>.
- [10] S. Mohapatra, G. Satapathy, S. P. Dash and P. R. Sahu, "Performance analysis of visible light communication system with imperfect CSI," *IEEE Commun. Lett.*, vol. 24, no. 12, pp. 2844-2848, Dec. 2020.
- [11] Y. Zeng, J. Xu and R. Zhang, "Energy minimization for wireless communication With rotary-Wing UAV," *IEEE Trans. Wireless Commun.*, vol. 18, no. 4, pp. 2329-2345, Apr. 2019.
- [12] T. Haarnoja, A. Zhou, P. Abbeel and S. Levine, "Soft actor-critic: Off-policy maximum entropy deep reinforcement learning with a stochastic actor," in *Proc. Int. Conf. Machine Learn.*, pp. 1861-1870, 2018.
- [13] C. Finn, P. Abbeel, and S. Levine, "Model-agnostic meta-learning for fast adaptation of deep networks," in *Proc. 34th Int. Conf. Machine Learn.*, pp. 1126-1135, 2017.
- [14] Y. Eghbali, *et al.*, "Beamforming for STAR-RIS-Aided Integrated Sensing and Communication Using Meta DRL," *IEEE Wireless Commun. Letts.*, vol. 13, no. 4, pp. 919-923, Apr. 2024.